Journal of the Ceramic Society of Japan 107 [6] 510-516 (1999) Paper

Structural Change Accompanying Crystallization in the Lithium Ion Conductive Li_2S–SiS_2–Li_3PO_4 Oxysulfide Glasses

Akitoshi HAYASHI, Kiyoharu TADANAGA, Masahiro TATSUMISAGO, Tsutomu MINAMI and Yoshinari MIURA*

Department of Applied Materials Science, Graduate School of Engineering, Osaka Prefecture University, 1-1, Gakuen-cho, Sakai-shi, Osaka 599-8531
**Department of Environmental Chemistry and Materials, Okayama University, 2-1-1, Tsushima-Naka, Okayama-shi 700-8530*

リチウムイオン伝導性 Li_2S–SiS_2–Li_3PO_4 系オキシスルフィドガラスの結晶化に伴う構造変化

林 晃敏・忠永清治・辰巳砂昌弘・南 努・三浦嘉也*

大阪府立大学大学院工学研究科・工学部機能物質科学科，599-8531 大阪府堺市学園町 1-1
*岡山大学環境理工学部，700-8530 岡山県岡山市津島中 2-1-1

The structural change of the $(100-x)(0.6Li_2S\cdot0.4SiS_2)\cdot xLi_3PO_4$ oxysulfide glasses during crystallization was analyzed by means of solid-state nuclear magnetic resonance (NMR) and X-ray photoelectron spectroscopy (XPS). The unique tetrahedral units of SiO_nS_{4-n} (n=1, 2, 3) and PO_nS_{4-n} (n=1, 2, 3) present in the glass samples vanished and the SiS_4, SiO_4, PS_4 and PO_4 units increased with proceeding of the crystallization process. Nonbridging sulfur and oxygen atoms decreased while bridging oxygens and S^{2-} increased with proceeding of the crystallization process. Large structural difference between the glass and the corresponding crystallized sample explained the high stability against crystallization found in the oxysulfide glass with the composition of x=5.
[Received October 5, 1998; Accepted March 26, 1999]

Key-words : *Crystallization, Glass, Lithium ion conductor, Thermal property, Solid-state NMR, XPS*

1. Introduction

Li_2S–SiS_2 glasses added with small amounts of Li_3PO_4 are promising for the application as solid electrolytes for the all-solid state lithium rechargeable battery because of their high conductivities of about 10^{-3} S·cm^{-1} at room temperature, wide electrochemical windows, and nonflammability.[1)-4)]

We have already reported the thermal properties of the $(100-x)(0.6Li_2S\cdot0.4SiS_2)\cdot xLi_3PO_4$ oxysulfide glasses.[2),3)] The addition of 5 mol% Li_3PO_4 brought about the improvement of the glass stability against crystallization, which decreased with a further addition of Li_3PO_4. In the case that the glass is easy to be crystallized, the structure of glass is expected to be similar to that of crystal precipitated from the glass. On the other hand, the structures of glass and crystal seem to be different in the case that the glass is not easy to be crystallized. The glass stability against crystallization, therefore, should closely relate to the degree of the structural change from glassy state to crystallized state.

The structure of these oxysulfide glasses was analyzed using solid-state nuclear magnetic resonance (NMR) and X-ray photoelectron spectroscopy (XPS). ^{29}Si and ^{31}P MAS NMR measurements revealed that most silicon and phosphorus atoms were coordinated with both sulfur and oxygen atoms in the glasses added with small amounts of Li_3PO_4.[5)] In the similar oxysulfide glasses added with small amounts of Li_4SiO_4 instead of Li_3PO_4, it was clarified from XPS measurements that sulfur atoms were mainly present as nonbridging ones while oxygen atoms were mainly present as bridging ones.[6),7)]

It is of great interest to investigate how the chemical bonds are rearranged during the crystallization of the oxysulfide glasses. In particular, it is very important to examine how the unique structural units composed of silicon and phosphorus atoms coordinated with both sulfur and oxygen atoms in the glasses are varied during the crystallization, since the silicon structural units with both sulfur and oxygen atoms are not known in crystals. Thus, the investigation on the structural change with the crystallization will provide the useful information about improving the glass stability against crystallization of the oxysulfide glasses.

In the present study, we first examine the behavior of crystallization in the $(100-x)(0.6Li_2S\cdot0.4SiS_2)\cdot xLi_3PO_4$ oxysulfide glasses. The crystallization temperature is determined using DTA measurements and the crystal phases precipitated from the glasses are identified using XRD measurements. The structural change of these oxysulfide glasses during the crystallization is analyzed by means of solid-state NMR and XPS measurements as comparing the structure of glass with that of corresponding crystals precipitated from the glass. Furthermore, the relationship between the degree of the structural change accompanying crystallization and the glass stability against crystallization is discussed.

2. Experimental

Reagent-grade chemicals of Li_2S, SiS_2 and Li_3PO_4 were used as starting materials. The mixture of these materials was placed in a carbon crucible and heated at 1000–1100°C for 2 h in a dry N_2-filled glove box ($[H_2O]<1$ ppm). The molten samples were rapidly cooled using a twin-roller quenching technique to prepare flakelike glasses of 20 μm in thickness.

DTA measurements were made under N_2 flow using a Rigaku Thermo-plus 8110 thermal analyzer in order to determine the crystallization temperature. The powdered glass samples sealed in an Al-pan were heated from room temperature to 550°C at a heating rate of 10°C/min and alumina powder was used as a reference material. In order to prepare crystallized samples, heat treatments were performed at 550°C for 1 h. X-ray diffraction analysis was carried out using a Shimadzu XRD-6000 diffractometer to

identify the precipitated crystal phases. The heat-treated powder samples were glued on a glass plate and covered with polyimide thin film in a N_2 atmosphere to avoid the attack of water and oxygen in air.

Solid-state ^{29}Si and ^{31}P MAS-NMR spectra were obtained using a Varian Unity Inova 300 NMR spectrometer. Detailed conditions for ^{29}Si and ^{31}P MAS-NMR were described in our previous paper.[8]

The XPS measurement was performed with a Fions Instrument S-probe ESCA (SSX100S) in a manner as described in our previous papers.[6),7)] Calibration of the spectra was done by setting the measured binding energy of the C1s peak to 284.4 eV of adventitious carbon accumulated in the analysis chamber of the spectrometer. The surface of samples was etched for 2 min using an Ar^+ ion gun in order to eliminate the impurities adsorped on the glass surface; it was confirmed that the etching caused no structural changes of the glasses.

3. Results

3.1 Thermal property and crystal phases precipitated from glasses

DTA measurements were carried out at a heating rate of 10°C/min for the $(100-x)(0.6Li_2S\cdot0.4SiS_2)\cdot xLi_3PO_4$ oxysulfide glasses in order to determine the glass transition temperature (T_g) and the crystallization temperature (T_c).

Figure 1 shows DTA curves for these oxysulfide glasses. The value of T_c-T_g, which is one of the measures of the glass stability, increases in the composition range up to $x=5$ and then decreases with an increase of x. The heat treatment of the oxysulfide glasses was performed at 550°C for 1 h in a dry N_2 atmosphere to prepare the crystallized samples; we chose the heat treatment temperature of 550°C because the crystallization was completed around 500°C in any composition. The crystal phases precipitated from these glasses were identified using X-ray diffraction measurements.

Figure 2 shows the X-ray diffraction patterns for the 80 $(0.6Li_2S\cdot0.4SiS_2)\cdot20Li_3PO_4$ oxysulfide samples before and after crystallization. Diffraction peaks due to the crystal phases of Li_2S, Li_4SiS_4, and Li_3PO_4 are observed in the crystallized sample while the halo pattern is observed in the glass sample. The precipitated crystal phases from the $(100-x)(0.6Li_2S\cdot0.4SiS_2)\cdot xLi_3PO_4$ oxysulfide glasses were listed in Table 1. The crystal phases described with bold characters are the main phases present in the crystallized samples. The main crystal phases precipitated were

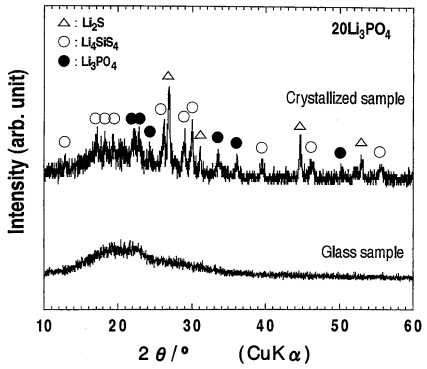

Fig. 2. X-ray diffraction patterns for the $80(0.6Li_2S\cdot0.4SiS_2)\cdot20Li_3PO_4$ oxysulfide glass before and after crystallization.

Table 1. Crystal Phases Precipitated from the $(100-x)(0.6Li_2S\cdot0.4SiS_2)\cdot xLi_3PO_4$ Oxysulfide Glasses Heat-Treated at 550°C for 1 h. The Crystal Phases Described with Bold Characters are the Main Phases Present in the Crystallized Samples

x / mol%	Crystal phase
0	**Li_4SiS_4**
5	**Li_4SiS_4** + Li_2S + unknown
10	**Li_2S + unknown** + Li_4SiS_4
20	**Li_2S** + Li_4SiS_4 + Li_3PO_4
40	**Li_3PO_4 + Li_2S** + Li_4SiS_4

Li_4SiS_4 at the compositions with $x=0$ and 5, Li_2S with $x=10$ and 20, and Li_3PO_4 with $x=40$.

3.2 ^{29}Si MAS-NMR spectra

The structural change around silicon atoms accompanying crystallization was examined by comparing the ^{29}Si MAS-NMR spectra for the glass samples with those of the crystallized samples. Figure 3 shows the ^{29}Si MAS-NMR spectra for the $80(0.6Li_2S\cdot0.4SiS_2)\cdot20Li_3PO_4$ oxysulfide glass before and after crystallization as an example. Six

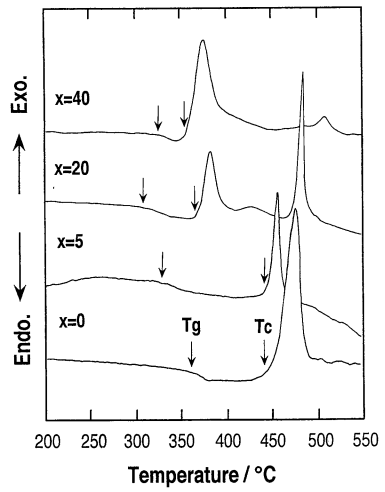

Fig. 1. DTA curves for the $(100-x)(0.6Li_2S\cdot0.4SiS_2)\cdot xLi_3PO_4$ oxysulfide glasses.

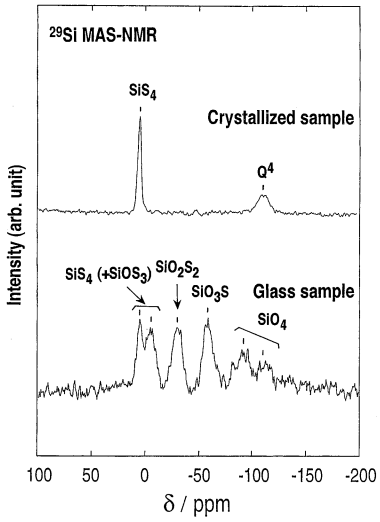

Fig. 3. ^{29}Si MAS-NMR spectra for the $80(0.6Li_2S\cdot0.4SiS_2)\cdot20Li_3PO_4$ oxysulfide glass before and after crystallization.

peaks at about 5, −3, −25, −55, −90 and −110 ppm are observed in the spectrum of the glass sample. However, four peaks at about −3, −25, −55 and −90 ppm completely disappear and only two peaks at 5 and −110 ppm remain in the spectrum of the crystallized sample.

The peak at 5 ppm is ascribed to silicon atoms coordinated with four sulfur atoms, which are represented as SiS_4 tetrahedral units; these SiS_4 units are connected each other only by corner-sharing or isolated SiS_4^{4-} ions.[9] The peak at −3 ppm is assigned to the combination of the following two silicon-centered tetrahedral units.[8] One is the SiS_4 units connected by both edge- and corner-sharing and the other is $SiOS_3$ tetrahedral units in which silicon atoms are coordinated with one oxygen and three sulfur atoms. The two peaks at −25 and −55 ppm are respectively assigned to SiO_2S_2 and SiO_3S units. The broad peaks at around −90 and −110 ppm are due to silicon atoms coordinated with four oxygen atoms, SiO_4 tetrahedral units.[10] These peaks are respectively due to Q^3 and Q^4 units using the Q^n nomenclature; Q means SiO_4 units and n indicates the number of bridging oxygen atoms.

In the glass sample, large amounts of SiO_nS_{4-n} (n=1, 2, 3) structural units in which silicon atoms are coordinated with both oxygen and sulfur atoms and SiS_4 units with edge-sharing are present. During the crystallization, these unique silicon structural units vanish because of the absence of the three peaks at −3, −25 and −55 ppm in the crystallized sample. The sharp peak at 5 ppm observed in the crystallized sample is due to isolated SiS_4^{4-} units because the crystal phase of Li_4SiS_4 was identified by XRD measurements at this composition. The broad peak at about −90 ppm disappears while the peak at about −110 ppm still remains in the crystallized sample. These changes suggest that the structural units of Q^3 being present in the glass sample vanish and only Q^4 units are present in the crystallized sample. In other words, all of the SiO_4 tetrahedral units in the crystallized samples are connected with each other by four bridging oxygen atoms, suggesting that the continuously connected SiO_4 network must be present as amorphous state.

Figure 4 shows the ^{29}Si MAS-NMR spectra for the $(100-x)(0.6Li_2S\cdot 0.4SiS_2)\cdot xLi_3PO_4$ oxysulfide glasses before and after crystallization in a wide range of x. In the glass samples, the intensity of the peaks at −25, −55, −90 and −110 ppm against the peaks at 5 and −3 ppm gradually increases with an increase of x. The intensity of the peak at −110 ppm against the peak at 5 ppm also increases with an increase of x in the crystallized samples. The peaks at −3, −25 and −55 ppm due to SiO_nS_{4-n} (n=1, 2, 3) units were observed at the composition with x=0, where oxygen atoms should not be present. This is probably caused by the fact that reagent-grade sulfide chemicals used as starting materials include small amounts of oxygen atoms as impurity.

These spectra were separated, by using a best-fit deconvolution program with Gaussian distribution functions, into several peaks due to silicon atoms coordinated with different numbers of sulfur atoms. The relative amounts of each silicon structural unit were calculated from the areas under each peak divided by the total area of all the separated peaks. In the present study, we have classified the six peaks observed in the glass samples into three silicon-centered structural groups; the peaks at 5 and −3 ppm belong to (a) SiS_4 (+$SiOS_3$) group, the peaks at −25 and −55 ppm to (b) SiO_2S_2+SiO_3S group, and the peaks at −90 and −110 ppm to (c) SiO_4 group, respectively. The peaks observed in the crystallized samples are also classified in the same manner.

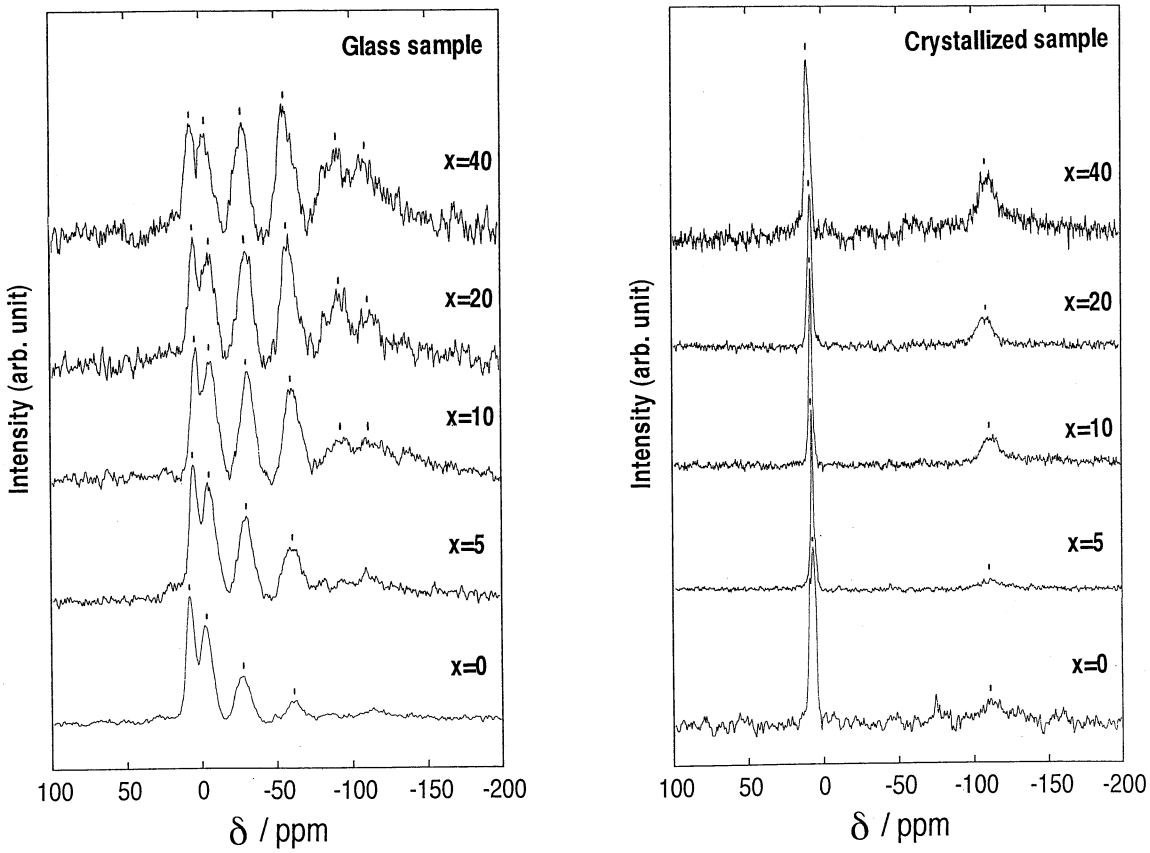

Fig. 4. ^{29}Si MAS-NMR spectra for the $(100-x)(0.6Li_2S\cdot 0.4SiS_2)\cdot xLi_3PO_4$ oxysulfide glasses before and after crystallization.

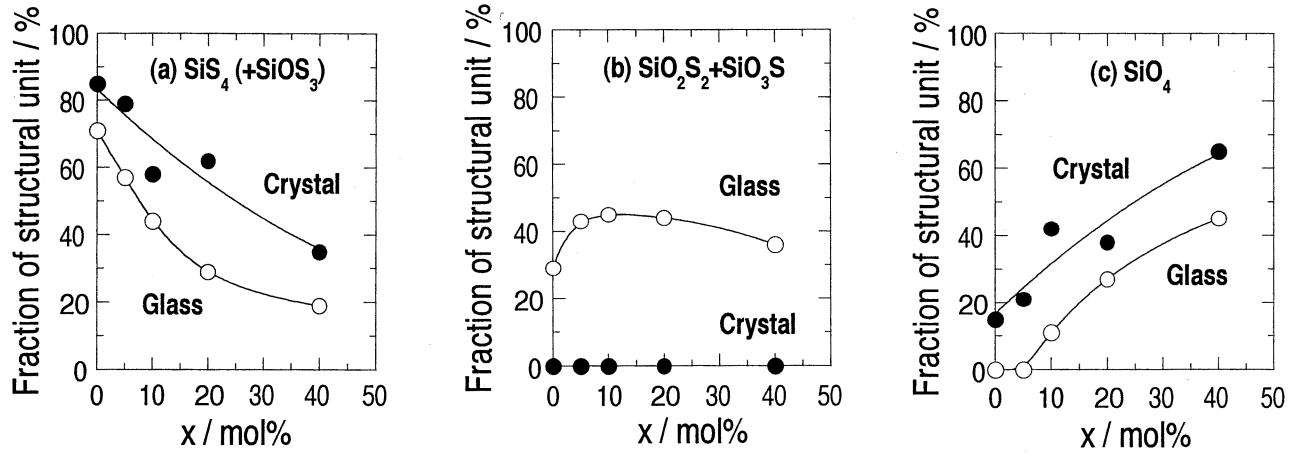

Fig. 5. Composition dependence of the fraction of several groups of silicon structural units for the $(100-x)(0.6Li_2S\cdot0.4SiS_2)\cdot xLi_3PO_4$ oxysulfide glasses before and after crystallization.

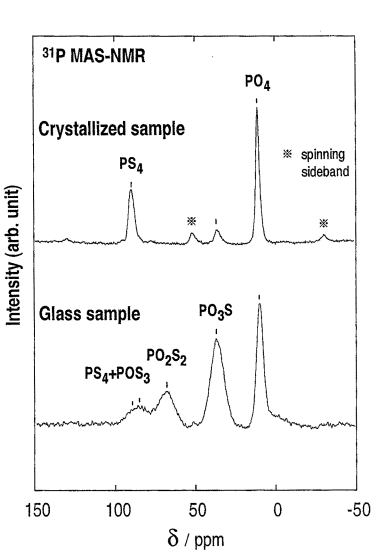

Fig. 6

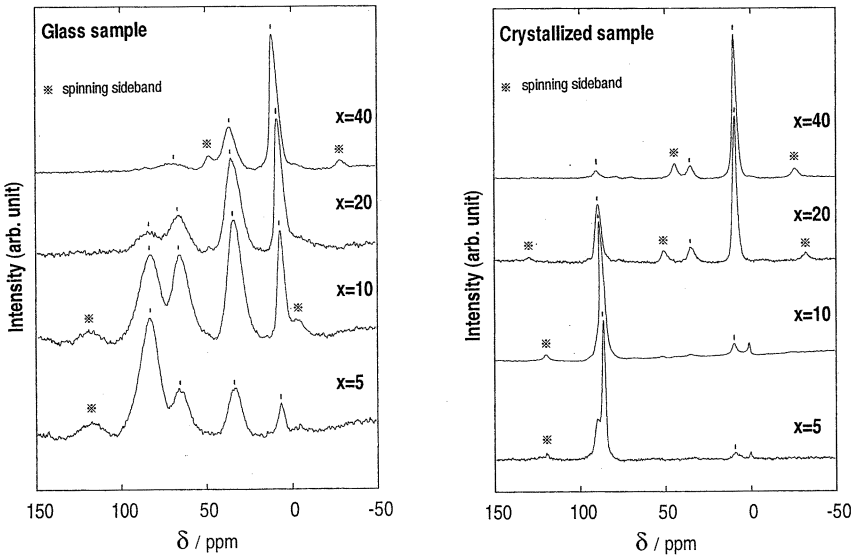

Fig. 7

Fig. 6. ^{31}P MAS-NMR spectra for the $80(0.6Li_2S\cdot0.4SiS_2)\cdot20Li_3PO_4$ oxysulfide glass before and after crystallization.
Fig. 7. ^{31}P MAS-NMR spectra for the $(100-x)(0.6Li_2S\cdot0.4SiS_2)\cdot xLi_3PO_4$ oxysulfide glasses before and after crystallization.

Figure 5 shows the composition dependence of the fraction of the three groups of silicon structural units, calculated from the deconvoluted peak area of the ^{29}Si NMR spectra, for the $(100-x)(0.6Li_2S\cdot0.4SiS_2)\cdot xLi_3PO_4$ oxysulfide glasses before and after crystallization. The open and closed circles respectively denote the glass and crystallized samples.

The SiS_4 (+$SiOS_3$) silicon structural units, as shown in Fig. 5(a), monotonously decrease with an increase of x in the glass samples. Similar composition dependence is observed in the crystallized samples; closed circles in this group represent the fraction of only SiS_4 units because only the peak at 5 ppm due to SiS_4 units is observed and the peak at −3 ppm partially due to $SiOS_3$ units disappears in the crystallized samples. In addition, the fraction of SiS_4 units in the crystallized samples is larger than that in the glass samples at a given composition.

The SiO_4 units monotonously increase with an increase of x in both glass and crystallized samples (Fig. 5(c)); closed circles in this group are attributable to only the fraction of Q^4 units because the peak at −110 ppm due to Q^4 units is only observed and the peak at −90 ppm due to Q^3 units disappears in the crystallized samples. The fraction of Q^4 units in the crystallized samples is larger than that in the glass samples at a given composition.

The fraction of Fig. 5(b) SiO_2S_2+SiO_3S units drastically increases with the addition of small amounts of Li_3PO_4 while that slightly decreases with the addition of large amounts of Li_3PO_4 in the glass samples; the fraction of these units is over 40% in the range $5\leq x\leq20$. These units are not present at any composition in the crystallized samples.

It is concluded that the SiS_4 structural units decrease, while SiO_4 units increase with an increase of x in both glass and crystallized samples. The SiO_nS_{4-n} ($n=1, 2, 3$) units present in the glass samples completely vanish and the SiS_4 and SiO_4 (especially Q^4) units increase during the crystallization at any composition.

3.3 ^{31}P MAS-NMR spectra

The structural change around phosphorus atoms accompanying crystallization was examined by comparing the ^{31}P MAS-NMR spectra of the glass samples with those of the crystallized samples. As an example, Fig. 6 shows the ^{31}P MAS-NMR spectra for the $80(0.6Li_2S\cdot0.4SiS_2)\cdot20Li_3PO_4$

oxysulfide glass before and after crystallization. Four peaks at about 82, 65, 34 and 8 ppm are observed in the spectrum of the glass sample. In the crystallized sample, the peaks at 87 and 8 ppm become sharper and stronger than those in the glass sample. The peaks at 65 and 34 observed in the glass sample almost disappear in the crystallized sample.

The sharp peak at 87 ppm observed in the crystallized sample is assigned to PS_4 units (isolated PS_4^{4-} units) on the basis of the ^{31}P NMR study for the Li_2S-P_2S_5 glasses by Eckert et al.[11] The broad peak at around 82 ppm observed in the glass sample has been assigned to the combination of PS_4 and POS_3 tetrahedral units in our previous paper.[8] The peaks at 65, 34 and 8 ppm are also assigned to PO_2S_2, PO_3S and PO_4 (isolated PO_4^{4-}) units, respectively.

In the glass sample, large amounts of PO_nS_{4-n} (n=1, 2, 3) structural units in which phosphorus atoms are coordinated with both oxygen and sulfur atoms are present. The crystallization brings about the disappearance of these unique phosphorus structural units. On the contrary, PS_4 and PO_4 units increase accompanying crystallization; an increase of PO_4 units corresponds to the formation of the crystal phase of Li_3PO_4 identified by XRD measurements at this composition.

Figure 7 shows the ^{31}P MAS-NMR spectra for the $(100-x)(0.6Li_2S\cdot0.4SiS_2)\cdot xLi_3PO_4$ oxysulfide glasses before and after crystallization in a wide range of x. In the glass samples, the intensity of the peak at 82 ppm monotonously decreases, while that at 8 ppm increases with an increase of x. The intensity of the peaks at 65 and 34 ppm increases and then decreases with an increase of x. In the crystallized samples, the intensity of the peak at 87 ppm decreases, while that at 8 ppm increases with an increase of x. There is an unknown peak at 0 ppm in the spectra for the crystallized samples at the compositions with x=5 and 10.

These spectra were separated, by using a best-fit deconvolution program with Gaussian distribution functions, into several peaks due to phosphorus atoms coordinated with different numbers of sulfur atoms. In the present study, we have classified these peaks observed in the glass and crystallized samples into three phosphorus structural groups; the peak at around 82 ppm in the glass samples and that at 87 ppm in the crystallized samples belong to (a) PS_4+POS_3 group, the peaks at 65 and 34 ppm to (b) $PO_2S_2+PO_3S$ group, and the peak at 8 ppm to (c) PO_4 group, respectively.

Figure 8 shows the composition dependence of the fraction of several groups of phosphorus structural units, calculated from the peak area of the ^{31}P NMR spectra, for the $(100-x)(0.6Li_2S\cdot0.4SiS_2)\cdot xLi_3PO_4$ oxysulfide glasses before and after crystallization. The open and closed circles respectively denote the glass and crystallized samples.

The phosphorus structural units, (a) PS_4+POS_3, decrease with an increase of x in the glass samples. Similar composition dependence is observed in the crystallized samples; closed circles in this group represent the fraction of only PS_4 units because the sharp peak at 87 ppm due to PS_4 units is observed in the crystallized samples instead of the broad peak at 82 ppm due to the combination of PS_4 and POS_3 units observed in the glass samples. The fraction of PS_4 units in the crystallized samples is larger than that in the glass samples at a given composition. The PO_4 units increase with an increase of x in both the glass and crystallized samples (Fig. 8(c)). The fraction of PO_4 units in the crystallized samples is larger than that in the glass samples at a given composition. The Fig. 8(b) $PO_2S_2+PO_3S$ units increase up to the composition with x=10 and then decrease with an increase of x in the glass samples. These units are not present in the crystallized samples at the composition up to x=10 although small amounts of these units remain at the composition with x=20 and 40.

It is concluded that the PS_4 silicon structural units decrease, while PO_4 units increase with an increase of x in both glass and crystallized samples. The PO_nS_{4-n} (n=1, 2, 3) units present in the glass samples almost vanish and the fraction of PS_4 and PO_4 units increase during the crystallization at any composition.

3.4 X-ray photoelectron spectra

The change of the bonding state of sulfur and oxygen atoms accompanying crystallization was examined by comparing the S2p and O1s photoelectron spectra of the glass samples with those of the crystallized samples.

Figure 9 shows the S2p photoelectron spectra for the 80 $(0.6Li_2S\cdot0.4SiS_2)\cdot20Li_3PO_4$ oxysulfide glass before and after crystallization. A maximum is observed at around 161 eV with a shoulder at around 162 eV in both spectra of glass and crystallized samples; a tail at a lower binding energy side is larger in the spectrum of crystallized sample. These spectra were deconvoluted in the same manner reported in our previous paper using a best-fit program with a combination of Gaussian (70%) and Lorentzian (30%).[6),7)] The spectra for both glass and crystallized samples in Fig. 9 can be separated into four components (a), (b), (c), and (d) on the basis of the spin-orbital splitting of sulfur atoms; the peaks (a) and (b) at the higher binding energy side are attributed to $S_{NB}2p_{1/2}$ and $S_{NB}2p_{3/2}$, respectively, while the peaks (c) and (d) at the lower side to $S^{2-}2p_{1/2}$ and $S^{2-}2p_{3/2}$,

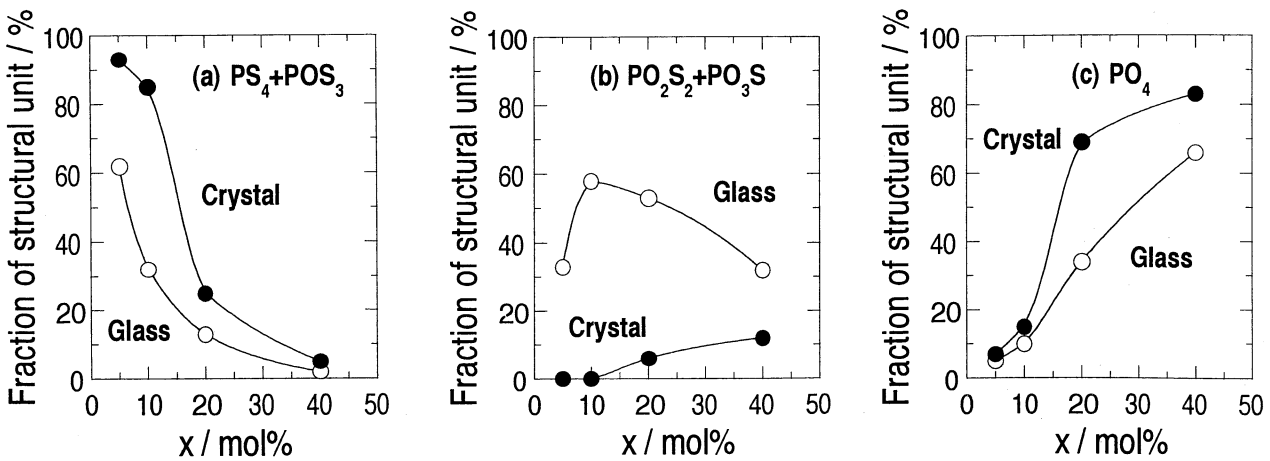

Fig. 8. Composition dependence of the fraction of several groups of phosphorus structural units for the $(100-x)(0.6Li_2S\cdot0.4SiS_2)\cdot xLi_3PO_4$ oxysulfide glasses before and after crystallization.

respectively. The symbol "S_{NB}" represents nonbridging sulfur atoms. The binding energies (BE) and the relative area of S2p peaks due to these four components are listed in Table 2. As the relative amounts of S_{NB} and S^{2-} are proportional to the corresponding S2p peak areas,[12),13)] the relative amounts of S^{2-} in the glass and crystallized samples are estimated to be 22 and 33%, respectively.

It is revealed from S2p spectra that both S_{NB} and S^{2-} are present in the $80(0.6Li_2S\cdot0.4SiS_2)\cdot20Li_3PO_4$ oxysulfide glass before and after crystallization and the relative amount of S^{2-} increases with the crystallization.

Figure 10 shows the O1s photoelectron spectra for the $80(0.6Li_2S\cdot0.4SiS_2)\cdot20Li_3PO_4$ oxysulfide glass before and after crystallization. Two peaks at around 532 and 530 eV are observed in both glass and crystallized samples. The intensity of the peak at 530 eV in the crystallized sample is weaker than that in the glass sample. These spectra were separated into two components (a) and (b) by using the best-fit deconvolution program on the basis of the XPS study for the Na_2O–P_2O_5 oxide glasses.[14),15)] The peak (a) at the higher binding energy side (532 eV) is attributed to bridging oxygen atoms (O_B) and the peak (b) at the lower binding energy side (530 eV) to the overlapping of nonbridging oxygen (O_{NB}) and double bonded oxygen atoms (O_D) which make P=O bonds. The binding energies and the relative area of O1s peaks due to these two components are listed in Table 3. The relative amounts of O_B and ($O_{NB}+O_D$) are respectively estimated to be 53 and 47% in the glass samples, while those are 69 and 31% in the crystallized samples.

O1s spectra revealed that O_B, O_{NB}, and O_D are present in the $80(0.6Li_2S\cdot0.4SiS_2)\cdot20Li_3PO_4$ oxysulfide glass before and after crystallization and the relative amount of O_B increases and that of ($O_{NB}+O_D$) decreases with the crystallization.

4. Discussion

4.1 Structural change accompanying crystallization in the $80(0.6Li_2S\cdot0.4SiS_2)\cdot20Li_3PO_4$ oxysulfide glass

In this section, the structural change with the crystallization is discussed for the $80(0.6Li_2S\cdot0.4SiS_2)\cdot20Li_3PO_4$ oxysulfide glass as an example using the structural data obtained in the previous sections.

Figure 2 revealed that the crystal phases of Li_2S, Li_4SiS_4, and Li_3PO_4 were present in the crystallized sample at this composition.

The S2p photoelectron spectra in Fig. 9 indicated that the nonbridging sulfur atoms decreased while S^{2-} increased with the crystallization. The O1s photoelectron spectra in Fig. 10 indicated that the nonbridging oxygen atoms decreased while bridging oxygen atoms increased with the crystallization. On the basis of such structural changes, the Li_2S crystal must be formed by the following reaction:

$$Si\text{-}S^{-}\cdots{}^{+}Li+Li^{+}\cdots{}^{-}O\text{-}Si\longrightarrow Si\text{-}O\text{-}Si+Li_2S \quad (1)$$

The fact that the crystallization brought about the increase of Q^4 units in Fig. 3, in which all of the SiO_4 tetrahedral units are connected each other by four bridging

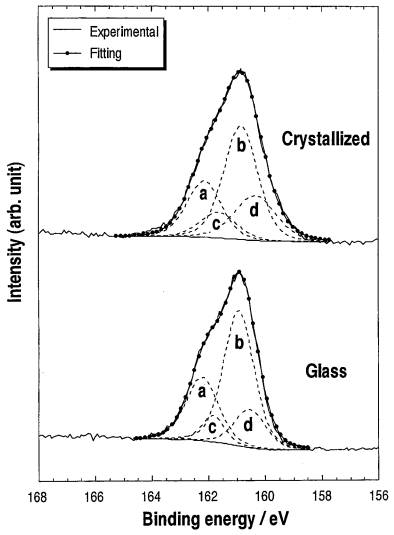

Fig. 9. S2p photoelectron spectra for the $80(0.6Li_2S\cdot0.4SiS_2)\cdot20Li_3PO_4$ oxysulfide glass before and after crystallization. The peaks of $S_{NB}2p_{1/2}$ and $S_{NB}2p_{3/2}$ are respectively denoted by the letter "a" and "b", and those of $S^{2-}2p_{1/2}$ and $S^{2-}2p_{3/2}$ are respectively denoted by "c" and "d".

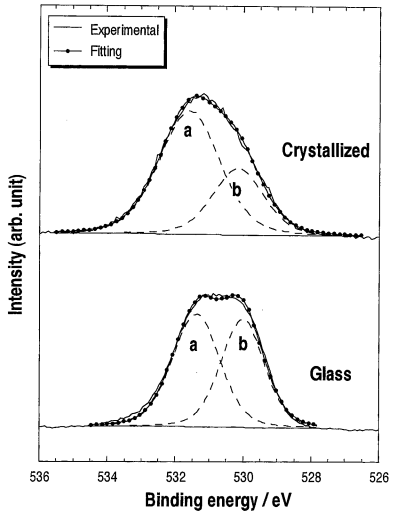

Fig. 10. O1s photoelectron spectra for the $80(0.6Li_2S\cdot0.4SiS_2)\cdot20Li_3PO_4$ oxysulfide glass before and after crystallization. The peaks of O_B and ($O_{NB}+O_D$) are respectively denoted by the letter "a" and "b".

Table 2. Binding Energies (BE) and the Relative Area of S2p Peaks Due to Four Components of $S_{NB}2p_{1/2}$, $S_{NB}2p_{3/2}$, $S^{2-}2p_{1/2}$ and $S^{2-}2p_{3/2}$ for the $80(0.6Li_2S\cdot0.4SiS_2)\cdot20Li_3PO_4$ Oxysulfide Glass before and after Crystallization

	$S_{NB}2p_{1/2}$		$S_{NB}2p_{3/2}$		$S^{2-}2p_{1/2}$		$S^{2-}2p_{3/2}$	
	BE (eV)	Area (%)	BE (eV)	Area (%)	BE (eV)	Area (%)	BE (eV)	Area (%)
Glass sample	162.3	26	161.0	52	161.9	7	160.6	15
Crystallized sample	162.2	22	160.9	45	161.7	11	160.4	22

Table 3. Binding Energies (BE) and the Relative Area of O1s Peaks Due to O_B and ($O_{NB}+O_D$) Components for the 80 $(0.6Li_2S\cdot0.4SiS_2)\cdot20Li_3PO_4$ Oxysulfide Glass before and after Crystallization

	O_B		$O_{NB}+O_D$	
	BE (eV)	Area (%)	BE (eV)	Area (%)
Glass sample	531.5	53	530.1	47
Crystallized sample	531.7	69	530.2	31

oxygen atoms supports this reaction in terms of forming Si–O–Si network.

The ^{29}Si MAS-NMR spectra in Fig. 3 also indicated that the unique SiO_nS_{4-n} ($n=1, 2, 3$) silicon structural units present in the glass sample completely vanished and the SiS_4 (isolated SiS_4^{4-}) and SiO_4 (Q^4) units increased with crystallization. These structural changes support the formation of the Li_4SiS_4 crystal by the following reactions:

$$2SiO_2S_2 \longrightarrow SiS_4+SiO_4 \quad (2)$$

$$SiOS_3+SiO_3S \longrightarrow SiS_4+SiO_4 \quad (3)$$

The ^{31}P MAS-NMR spectra in Fig. 6 also indicated that the unique PO_nS_{4-n} ($n=1, 2, 3$) phosphorus structural units present in the glass sample almost disappeared and the PO_4 (isolated PO_4^{4-}) and PS_4 units increased with crystallization. These structural changes support the formation of the Li_3PO_4 crystal by the following reactions:

$$2PO_2S_2 \longrightarrow PS_4+PO_4 \quad (4)$$

$$POS_3+PO_3S \longrightarrow PS_4+PO_4 \quad (5)$$

At the other compositions in the $(100-x)(0.6Li_2S\cdot 0.4SiS_2)\cdot xLi_3PO_4$ oxysulfide glasses, the structural change accompanying crystallization seems to be brought about with the same reaction represented by Eqs. (1)–(5).

4.2 Relationship between the degree of the structural change accompanying crystallization and glass stability against crystallization

In this section, the relationship between the degree of the structural change accompanying crystallization and T_c-T_g which is one of the measures of glass stability against crystallization is discussed in the $(100-x)(0.6Li_2S\cdot 0.4SiS_2)\cdot xLi_3PO_4$ oxysulfide glasses.

Although the multiple crystallization was observed in the DTA curves for the oxysulfide glasses in Fig. 1, the mainly precipitated crystal phases in the samples heat-treated at 550°C for 1 h should be the first precipitated crystal phase, which directly affects the value of the T_c and T_c-T_g. In the case that the structure of glass is similar to that of the crystal precipitated mainly from the glass, the value of T_c-T_g must be low because large structural change like exchange of chemical bonds and migration of atoms is not needed during the crystallization. On the other hand, the value of T_c-T_g must be high in the case that the structures of glass and crystal are considerably different because large structural change is necessary for crystallization.

The glass with $x=5$ exhibited high T_c-T_g as shown in Fig. 1. The crystal phase of Li_4SiS_4 was mainly precipitated from the glass at this composition. The results of ^{29}Si NMR measurements revealed that the structural change with rearrangement of chemical bonds, i.e., transformation of a number of the SiO_nS_{4-n} ($n=1, 2, 3$) units and SiS_4 units with edge-sharing to the isolated SiS_4^{4-} units, occurred during the crystallization to form the crystal phase of Li_4SiS_4. Because large structural change is actually brought about during the crystallization, the glass at this composition must have exhibited high glass stability against crystallization.

On the other hand, the glass with $x=40$ exhibited low T_c-T_g as shown in Fig. 1. The crystal phase of Li_3PO_4 was mainly precipitated from the glass at this composition. A number of isolated PO_4^{4-} units which are needed to form the Li_3PO_4 crystal have already been present in the glass structure. Large structural change did not occur during the crystallization at this composition because the structure of the glass was very similar to that of the mainly precipitated crystal phase. Therefore, the glass at this composition exhibited low glass stability against crystallization.

5. Conclusions

Crystallization behavior of the $(100-x)(0.6Li_2S\cdot 0.4SiS_2)\cdot xLi_3PO_4$ oxysulfide glasses was examined. The value of T_c-T_g, which is one of the measures of the glass stability, increased in the composition range up to $x=5$ and then decreased with an increase of x. The mainly precipitated crystal phases were Li_4SiS_4 at the composition with $x=0$ and 5, Li_2S with $x=10$ and 20, and Li_3PO_4 with $x=40$.

Solid-state NMR spectra indicated that the unique tetrahedral units of SiO_nS_{4-n} ($n=1, 2, 3$) and PO_nS_{4-n} ($n=1, 2, 3$) present in the glass samples vanished and the SiS_4, SiO_4 (especially Q^4), PS_4 and PO_4 units increased with the crystallization at any composition. X-ray photoelectron spectra of the samples with $x=20$ revealed that nonbridging sulfur and oxygen atoms decreased, while bridging oxygen and S^{2-} increased with the crystallization. We proposed a series of reactions representing the structural change from the glass to the precipitated crystal phase.

The glass stability against crystallization must be correlated with the similarity of the structures of the glasses and corresponding crystallized samples. The structure of the glass with $x=5$ exhibiting high glass stability against crystallization is considerably different from that of the mainly precipitated crystal phase. The high stability against crystallization of this glass is probably caused by the fact that the large structural change is needed during the crystallization.

Acknowledgments This work was supported by the "Research for the Future" Program from the Japan Society for the Promotion of Science.

References

1) S. Kondo, K. Takada and Y. Yamamura, *Solid State Ionics*, **53–56**, 1183–86 (1992).
2) M. Tatsumisago, K. Hirai, T. Minami, K. Takada and S. Kondo, *J. Ceram. Soc. Japan*, **101**, 1315–17 (1993).
3) M. Tatsumisago, K. Hirai, T. Hirata, M. Takahashi and T. Minami, *Solid State Ionics*, **86–88**, 487–90 (1996).
4) K. Takada, N. Aotani, K. Iwamoto and S. Kondo, *Solid State Ionics*, **86–88**, 877–82 (1996).
5) K. Hirai, M. Tatsumisago, M. Takahashi and T. Minami, *J. Am. Ceram. Soc.*, **79**, 349–52 (1996).
6) A. Hayashi, M. Tatsumisago, T. Minami and Y. Miura, *J. Am. Ceram. Soc.*, **81**, 1305–09 (1998).
7) A. Hayashi, M. Tatsumisago, T. Minami and Y. Miura, *Phys. Chem. Glasses*, **39**, 145–50 (1998).
8) A. Hayashi, R. Araki, K. Tadanaga, M. Tatsumisago and T. Minami, *Phys. Chem. Glasses*, **40**, 140–45 (1999).
9) H. Eckert, J. H. Kennedy, A. Pradel and M. Ribes, *J. Non-Cryst. Solids*, **113**, 287–93 (1989).
10) A.-R. Grimmer, M. Mägi, M. Hähnert, H. Stade, A. Samoson, W. Wieker and E. Lippmaa, *Phys. Chem. Glasses*, **25**, 105–09 (1984).
11) H. Eckert, Z. Zhang and J. H. Kennedy, *Chem. Mater.*, **2**, 273–79 (1990).
12) J. Heo, J. S. Sanghera and J. D. Mackenzie, *J. Non-Cryst. Solids*, **101**, 23–30 (1988).
13) R. M. Almeida, H. Nasu, J. Heo and J. D. Mackenzie, *J. Mater. Sci. Lett.*, **6**, 701–04 (1987).
14) R. Gresch, W. Müller-Warmuth and H. Dutz, *J. Non-Cryst. Solids*, **34**, 127–36 (1979).
15) R. K. Brow, D. R. Tallant, J. J. Hudgens, S. W. Martin and A. D. Irwin, *J. Non-Cryst. Solids*, **177**, 221–28 (1994).